ARTICLE

OBC
www.rsc.org/obc

Oligonucleotides incorporating 8-aza-7-deazapurines: synthesis and base pairing of nucleosides with nitrogen-8 as a glycosylation position †

Junlin He and Frank Seela *
Laboratorium für Organische und Bioorganische Chemie, Institut für Chemie, Fachbereich Biologie/Chemie, Universität Osnabrück, Barbarastr. 7, D-49069 Osnabrück, Germany. E-mail: Frank.Seela@uni-osnabrueck.de

Received 10th February 2003, Accepted 3rd April 2003
First published as an Advance Article on the web 22nd April 2003

Oligonucleotides incorporating the unusually linked 8-aza-7-deazapurine N^8-(2′-deoxyribonucleosides) **3a**,**b** (purine and 6-amino-2-chloropurine analogues) were used as chemical probes to investigate the base pairing motifs of the universal nucleoside 8-aza-7-deazapurin-6-amine N^8-(2′-deoxyribofuranoside) **2** (adenine analogue) and that of the 2,6-diamino compound **1**. Owing to the absence of an amino group on the nucleoside **3a** the low stability of oligonucleotide duplexes incorporating this compound opposite to the four canonical DNA-constituents indicate hydrogen bonding and base pairing for the universal nucleosides **1** and **2** which form much more stable duplexes. When the 6-amino-2-chloro-8-aza-7-deazapurine nucleoside **3b** replaces **1** and is located at the same positions, two sets of duplexes are formed (i) high T_m duplexes with **3b** located opposite to dA or dC and (ii) low T_m duplexes with **3b** located opposite to dG or dT. These results are due to the steric clash of the 2-chloro substituent of **3b** with the 2-oxo group of dT or the 6-oxo group of dG while the 2-halogeno substituents are well accommodated in the base pairs formed with dA or dC. For comparison duplexes incorporating the regularly linked nucleosides **4**–**6a**,**b** containing the same nucleobases as those of **1**–**3a**,**b** were studied.

Introduction

A universal nucleoside is a compound containing a base which hybridizes equally well with all four constituents of DNA or RNA without significant destabilization of a nucleic acid duplex. The 8-aza-7-deazaadenine N^8-deoxyribonucleosides **1**[1,2] and **2**[3] (Scheme 1) show ambiguous base pairing when incorporated in oligonucleotide duplexes opposite to the four canonical DNA-constituents. Bidentate base pair motifs have been suggested to explain this behavior.[2] The duplex stabilization of these nucleosides is considered to be *via* hydrogen bonding as well as by stacking forming novel base pairs which are different from those formed by regularly linked nucleosides. As it was difficult to detect hydrogen bonds by NMR spectroscopy the problem was approached using the 8-aza-7-deazapurine nucleosides **3a**,**b** (purine numbering is used throughout the Discussion) as structural probes. Owing to the absence of amino groups of compound **3a** or the presence of the bulky 2-chloro substituent of compound **3b**, oligonucleotide duplexes incorporating these residues are expected to be less stable than those containing the universal nucleoside **2** (adenine analogue) or compound **1** (2,6-diaminopurine analogue). For this aim the phosphoramidites of compound **3a**,**b** were synthesized and the base pair stabilities of oligonucleotide duplexes incorporating compounds **1**–**3a**,**b** were studied. Oligonucleotides incorporating nucleosides **1** or **2** have been synthesized earlier,[1,3] while the syntheses of those incorporating compounds **3a**,**b** were performed using the newly synthesized phosphoramidites **14a**,**b**. The stabilities of duplexes incorporating the unusually linked nucleosides **3a**,**b** were compared with those containing the regularly linked nucleosides **6a**,**b**.[4–6] The data will show that compounds **1** and **2** are expected to form H-bonded base pairs with the four canonical DNA-constituents which are not only stabilized by stacking interactions as in **3a**; oligomers incorporating **3b** form two sets of base pairs with high and low stability relative to those formed by the nucleosides **1** and **2**.

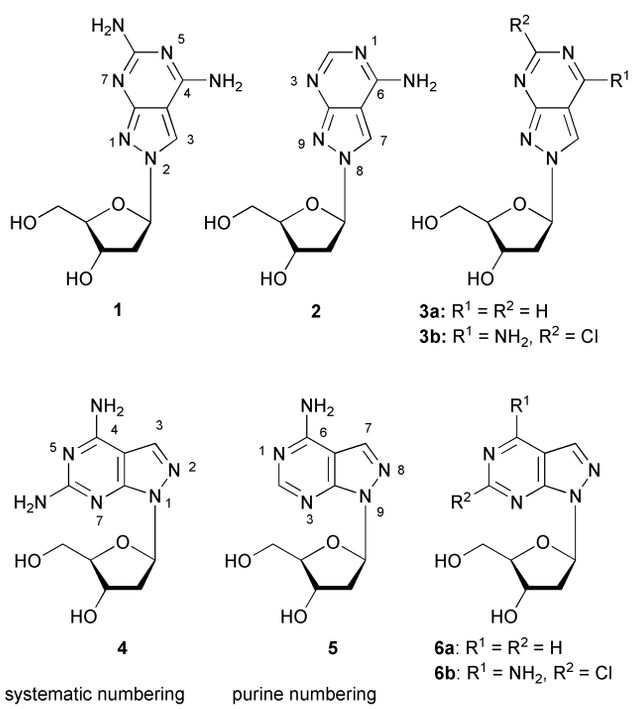

Scheme 1 Regularly and unusually linked nucleosides.

Results and discussion

Monomers

The nucleosides **1**,[3] **2**,[1,7] **4**,[3] **5**,[1,7] and **6a**,**b**,[4,5,6] were already synthesized, but **6a**,**b** were not studied in the context of oligonucleotide incorporation. Compounds **3a** and **6a** were obtained from nucleobase anion glycosylation[1] of **8a**[4] with 2-deoxy-3,5-

† Electronic supplementary information (ESI) available: The molecular weight of oligonucleotides measured by MALDI-TOF. See http://www.rsc.org/suppdata/ob/b3/b301608k/

DOI: 10.1039/b301608k

Table 1 ^{13}C NMR Chemical shifts of pyrazolo[3,4-*d*]pyrimidine 2′-deoxyribonucleosides and derivatives thereof[a]

	C(2)[b,c] C(6)[c,d]	C(4)[b,c] C(7a)[c,d]	C(5)[b] C(3a)[d]	C(6)[b,c] C(4)[c,d]	C(7)[b] C(3)[d]	C(1′)	C(2′)	C(3′)	C(4′)	C(5′)
3a	156.6	155.3	112.2	157.9	125.3	91.2	[e]	70.0	88.6	61.4
3b	160.3	158.0	99.8	160.4	125.2	90.6	[e]	70.6	88.4	62.0
6a	153.3	152.3	114.7	155.1	134.3	83.7	37.9	70.9	87.7	62.2
6b	157.5	154.6	99.4	158.5	133.5	83.8	37.8	70.9	87.6	62.3
8b	157.0	155.7	100.8	163.1	132.0					
10a	156.9	155.6	112.3	158.1	126.4	91.0	37.2	74.5	82.6	64.0
10b	161.3	156.5	102.4	165.3	126.9	91.6	38.0	72.6	83.3	64.5
11a	157.0	155.6	112.3	158.1	134.2	91.0	37.3	74.6	82.6	64.0
11b	156.8	156.0	103.0	157.4	134.2	85.2	[e]	73.0	82.5	64.8
12a	156.6	155.3	112.3	157.9	125.8	90.8	[e]	70.1	86.3	63.7
12b	157.6	157.8	106.7	161.0	125.9	90.6	[e]	70.3	88.4	61.7
12c	157.5	157.8	106.9	161.1	126.0	86.0	[e]	70.1	90.1	63.6
13a	153.3	155.1	114.7	155.1	134.1	83.7	[e]	70.6	85.4	64.2
13b	156.9	155.3	106.7	158.5	134.1	83.8	37.7	70.9	87.6	62.3
13c	156.9	155.3	106.8	158.4	133.9	83.8	38.0	70.6	85.4	64.2

[a] Measured in (d_6)DMSO at 303 K. [b] Purine numbering. [c] Tentative. [d] Systematic numbering. [e] Superimposed by (d_6)DMSO.

di-*O*-(*p*-toluoyl)-*α*-D-*erythro*-pentofuranosyl chloride **9**[8] in the presence of KOH–TDA-1 in MeCN (Scheme 2). The protected regioisomers **10a** and **11a** were deblocked with 0.1 M sodium isopropoxide/ isopropanol yielding the nucleosides **3a** and **6a**. Similarly, the nucleosides **3b** and **6b** were synthesized by glycosylation of 2-chloro-6-isopropoxy-8-aza-7-deazapurine **8b** which was prepared from 2, 6-dichloropurine **7**[9] and subsequent ammonolysis (RT). The 6-amino groups of **3b** and **6b** were protected with di-(n-butyl)methylidene or dimethylmethylidene residues to form compounds **12b** and **13b**. The 5′-hydroxyl groups of compounds **3a**, **6a**, **12b**, **13b** were blocked with $(MeO)_2$Tr-residues (⟶ **12a**,**13a** and **12c**,**13c**). Phosphitylation under standard conditions afforded the phosphoramidites **14a**,**15a** and **14b**,**15b** (Scheme 3).[10]

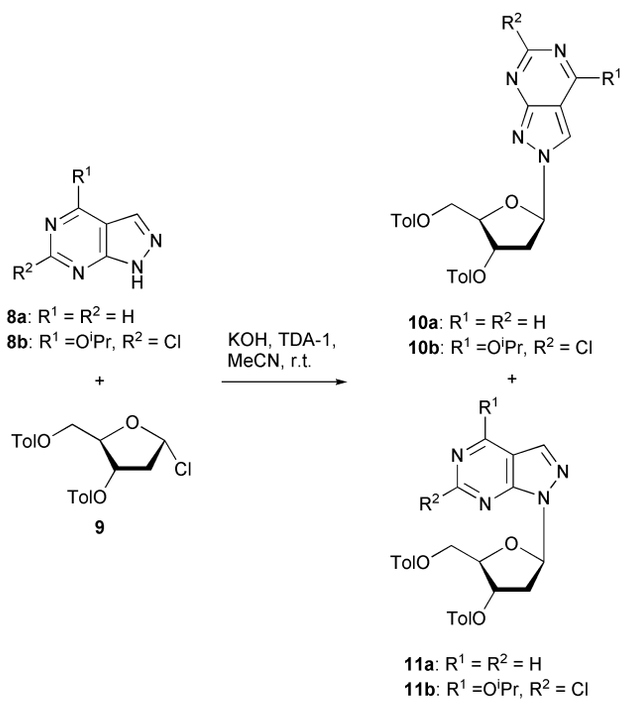

Scheme 2 Nucleobase anion glycosylation.

All compounds were characterized by NMR spectroscopy and elemental analysis (see Experimental section and Table 1). The assignment of the glycosylation position was performed on the basis of chemical shift analyses. The ^{13}C NMR chemical shifts are diagnostic and identify the regioisomers shown in Table 1. The carbon signals next to the glycosylation position are shifted by about 10 ppm upfield when the glycosylation

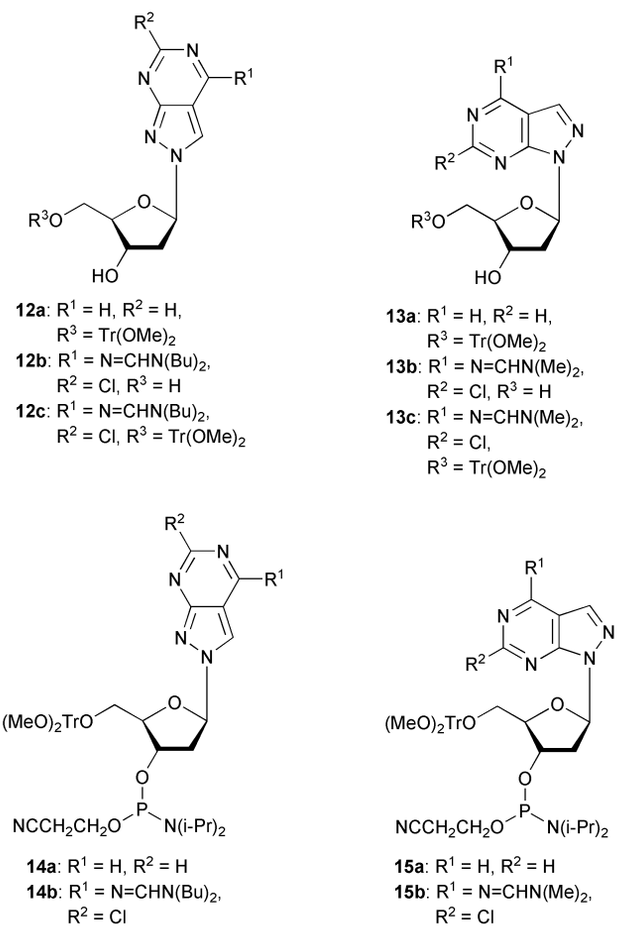

Scheme 3 Synthetic intermediates leading to phosphoramidites.

position moves from N(9) *e.g.* in compounds **6a**,**b** to N(8) *e.g.* for **3a**,**b**. This is also the case for the corresponding derivatives.

NOE data were used for the assignment of the anomeric configuration as well as for the glycosylation position of nucleosides **3a**,**b**. Irradiation of **3a** on H-(1′) (Scheme 4a) resulted in NOEs at H-(7) (6.6%) and H-(2′-*β*) (3.8%); irradiation on H-(7) (Scheme 4b) gave NOEs at H-(1′) (4.4%), H-(2′-*α*) (1.5%), and H-(6) (2%). Based on the spatial relationships of the H-atoms, the glycosylic bond of compound **3a** is *β*-D, and the sugar is attached at nitrogen-8. Similar data were also observed upon irradiation of H-C(1′) and H-C(7) of the N[8]-linked nucleoside **3b** showing *β*-D configuration (Scheme 4c,d). The structures of the nucleosides **3a** and **6a** were also confirmed by single crystal X-ray analyses (Fig. 1).[11] Both

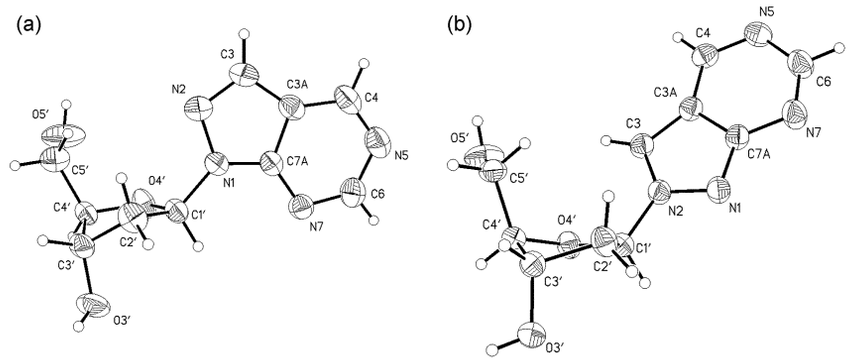

Fig. 1 Single crystal X-ray structures[11] of the nucleosides **6a** (left) and **3a** (right) (systematic numbering).

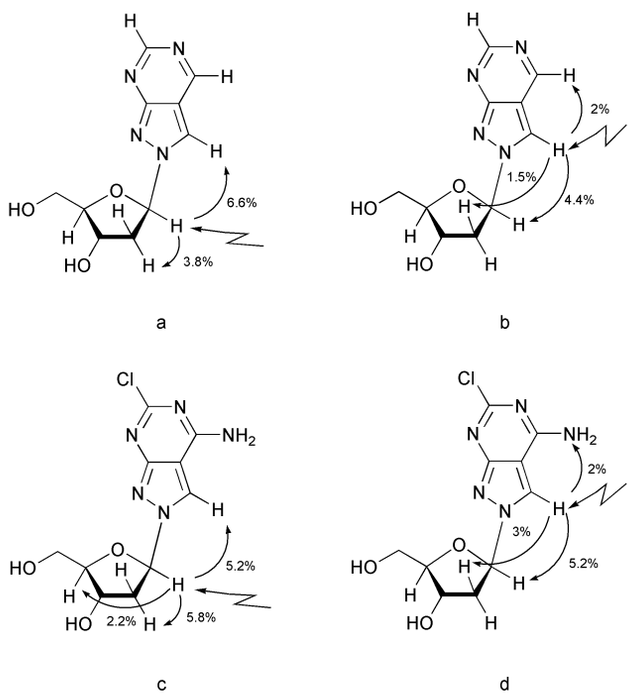

Scheme 4 NOE Data of the nucleosides **3a** (a, b) and **3b** (c, d).

nucleosides show an *anti* conformation around the *N*-glycosylic bond with $\chi = 15.0°$ (**3a**) and $-100.4°$ (**6a**), and an *S*-type sugar pucker (3′-*exo* for **3a** and C2′-*endo*-C3′-*exo* for **6a**). An *S*-type sugar pucker is typical for other 2′-deoxyribonucleosides.[12]

Oligonucleotides

1. Synthesis. The oligonucleotides were prepared by solid-phase synthesis. Phosphoramidite chemistry was employed with the tac-[4-(*tert*-butyl)phenoxyacetyl]-protected building blocks of dA, dG and dC. Because of stability problems of the nucleosides **3a**,**b** and **6a**,**b** at elevated temperature the deprotection of oligomers was performed in conc. aq. ammonia (25%) at room temperature for three hours. Reversed phase HPLC was used for the purification (see Experimental section). MALDI-TOF spectrometry was used for the characterization of all the oligonucleotides (Table S8, see Electronic supplementary information †).

2. Base pairing of 1–6 with dT in non-self-complementary duplexes. At first, the nucleosides **1** and **2** were incorporated into the non-self-complementary duplex (**16**·**17**) in place of dA. A single incorporation results in an almost identical T_m decrease ($\triangle T_m = -6$ °C, Table 2) in both cases.[2,3] When compound **3a** which does not contain an amino group replaced dA, the T_m decrease was −11 °C (Table 2). A similar strong decrease (−10 °C) was also found for compound **3b** which contains the 6-amino group but carries a bulky 2-chloro substituent. The same effect was observed when the replacement was made at another position (Table 2). The duplexes containing an abasic residue (S) (1,2-dideoxyribose)[2] gave the least stable duplexes with a T_m decrease of −17 °C.

The findings reported above (for **3a** and **3b**) indicate the formation of hydrogen bonds between the 6-amino group of **1** or **2** as proton donors and the 4-oxo of dT as a proton acceptor (see base pair motifs **I** and **IIa**) (Scheme 5).[2] Although compound **3b** contains a 6-amino group, it shows a low base pair stability (−10 °C for **3b**-dT replacement). This is due to the presence of the bulky 2-chloro substituent causing a steric clash between this substituent and the 4-oxo group of dT (base pair motif **IIb**, Scheme 5). Such a steric problem also arises from the presence of the 2-amino group of nucleoside **2** which contributes very little to the base pair stability with dT which is expected to form a much more stable base pair.

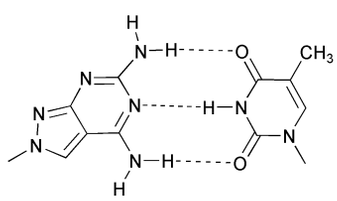

I: **1**-dT

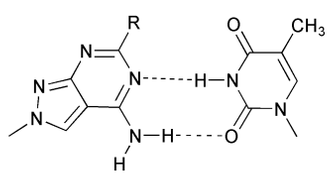

IIa: **2** - dT; R = H
IIb: **3b**-dT; R = Cl

Scheme 5 Base pair motifs **I** and **IIa**,**b**.

The base pairs formed between the regularly linked nucleosides **6a**,**b** with dT (Table 3) also show a decrease of the duplex stability because of the absence of a 6-amino group in **6a** and the bulky 2-chloro substituent in **6b**. There is no change of the T_m values with four or even six incorporations in the case of **5**-dT pairs.[13] The 2-amino group of nucleoside **4** contributes also very little to the base pair stability due to steric problem within the minor groove[14,15] Also the parent dA–dT base pair is sensitive to substitution of the 2-position on the adenine moiety. This has already been demonstrated on oligonucleotide duplexes incorporating 2-chloro-2′-deoxyadenosine opposite to dT[16] which show significantly lower T_m values than those containing dA. Apparently, the narrow minor groove can not well accommodate bulky substituents in the 2-position leading to less stable base pairs (base pair **IIIa**, Scheme 6). Also the 2-amino group of a 2,6-diaminopurine nucleoside (n^{2}A) shows

Table 2 T_m Values and thermodynamic data of duplex formation of oligonucleotides containing the nucleosides **1**–**3a**,**b** opposite to dT [a]

Duplex	T_m/°C	$\Delta H°$/kcal mol^{-1}	$\Delta S°$/cal mol^{-1} K^{-1}	$\Delta G°_{310}$/kcal mol^{-1}
5′-d(TAG GTC AAT ACT) (**16**) 3′-d(ATC CAG TTA TGA) (**17**)	50	−90	−252	−12.0
5′-d(TAG GTC A**1**T ACT) (**18**) 3′-d(ATC CAG TTA TGA) (**17**)	44	−82	−233	−9.6
5′-d(TAG GTC A**2**T ACT) (**19**) 3′-d(ATC CAG TTA TGA) (**17**)	43	−74	−210	−9.1
5′-d(TAG GTC A**3a**T ACT) (**20**) 3′-d(ATC CAG TTA TGA) (**17**)	39	−79	−225	−8.6
5′-d(TAG GTC A**3b**T ACT) (**21**) 3′-d(ATC CAG TTA TGA) (**17**)	40	−76	−216	−8.4
5′-d(TAG GTC AAT ACT) (**16**) 3′-d(ATC C**1**G TTA TGA) (**22**)	46	−88	−249	−10.1
5′-d(TAG GTC AAT ACT) (**16**) 3′-d(ATC C**2**G TTA TGA) (**23**)	46	−76	−212	−9.9
5′-d(TAG GTC AAT ACT) (**16**) 3′-d(ATC C**3a**G TTA TGA) (**24**)	40	−65	−180	−8.6
5′-d(TAG GTC AAT ACT) (**16**) 3′-d(ATC C**3b**G TTA TGA) (**25**)	39	−80	−231	−8.2

[a] Data measured at 260 nm in 1 M NaCl, 100 mM $MgCl_2$, and 60 mM Na-cacodylate buffer (pH 7.0) with 5 μM + 5 μM oligonucleotide.

Table 3 T_m Values and thermodynamic data of duplex formation of oligonucleotides containing multiple incorporations of the nucleosides **3a**,**b** and **6a**,**b** against dT [a]

Duplex	T_m/°C	$\Delta H°$/kcal mol^{-1}	$\Delta S°$/cal mol^{-1} K^{-1}	$\Delta G°_{310}$/kcal mol^{-1}
5′-d(TAG GTC A**3a**T ACT) (**20**) 3′-d(ATC C**3a**G TTA TGA) (**24**)	26	−75	−224	−5.4
5′-d(TAG GTC A**3b**T ACT) (**21**) 3′-d(ATC C**3b**G TTA TGA) (**25**)	23	−63	−188	−5.0
5′-d(TAG GTC **3a3a**T ACT) (**26**) 3′-d(ATC C**3a**G TT**3a** TGA) (**27**)	—			
5′-d(TAG GTC A**6a**T ACT) (**28**) 3′-d(ATC C**6a**G TTA TGA) (**29**)	28	−63	−185	−5.9
5′-d(TAG GTC A**6b**T ACT) (**30**) 3′-d(ATC C**6b**G TTA TGA) (**31**)	36	−76	−220	−7.7
5′-d(TAG GTC **6a6a**T ACT) (**32**) 3′-d(ATC C**6a**G TT**6a** TGA) (**33**)	15	−55	−164	−4.1
5′-d(TAG GTC **6b6b**T ACT) (**34**) 3′-d(ATC C**6b**G TT**6b** TGA) (**35**)	22	−70	−212	−4.7

[a] Data measured at 260 nm in 0.1 M NaCl, 10 mM $MgCl_2$, and 10 mM Na-cacodylate buffer (pH 7.0), with 5 μM + 5 μM oligonucleotide concentration.

similar behavior to nucleoside **4** and has only little influence on the expected higher base pair stability (base pair **IIIb**, Scheme 6).[17] The expected positive effect of a third hydrogen bond is neutralized by the negative steric clash of the 2-substituent. This is in accordance with the base pair motifs **IVa** for **6b**-dT and **IVb** for **4**-dT (Scheme 6, Tables 2 and 3).

The destabilization of the unusually linked nucleoside **3a** is stronger than that of the regularly linked compound **6a** indicating that the latter develops better stacking interactions. This behavior is different from regioisomeric indazole nucleosides.[18] In this case the regioisomers cause similar duplex stabilization also *via* base stacking. The different behavior of 8-aza-7-deaza-purine (pyrazolo[3,4-*d*]pyrimidine) nucleosides and indazole nucleosides might result from the electronic properties of the pyrimidine system (**3a** and **6a**) compared to the phenyl ring system of the indazole nucleosides. Multiple incorporation of the regularly linked nucleosides **6a**,**b** result generally in more stable duplexes than those containing **3a**,**b** (Table 3).

It was of interest to investigate the stacking of compounds **3a** and **6a** in cases when these molecules have maximal steric freedom. This was done by locating them at the 5′-terminus of an oligonucleotide duplex as dangling ends.[19] For this aim the oligonucleotides **36** and **37** were synthesized (Table 4). When these compounds were hybridized with oligonucleotide **17**, both compounds, **3a** as well as **6a**, increase the T_m value of the control duplex from 47 °C to 49 °C. This positive effect is in contrast to the negative influence of these nucleosides when they are incorporated in a central position of an oligonucleotide duplex (Table 3). The greater steric freedom at the end of a duplex gives the nucleobases the opportunity to optimize their stacking interactions with the nearest neighbors without disturbing the helical structure.

3. The ability of compounds 1–3a,b to act as universal nucleosides. Previous work on the N-8 glycosylated nucleosides **1** and **2** have shown that they can act as universal nucleosides.[3] Their behavior is different from that of the N-9 counterparts which do not show ambiguous base pairing.[3] Due to the almost identical stabilities of the duplexes and their high T_m values, it was suggested that compounds **1** and **2** form bidentate base pairs with all four canonical nucleosides. Within these base pairs the amino groups of **1** or **2** are always involved in hydrogen bonding, as shown in base pair motifs **VIa**,**b** (against dC), **VIIa**,**b** (against dA, Hoogsteen pair), **VIIIa**,**b** (against dA, purine "Watson-Crick" pair) and **IXa**,**b** (against dG, purine "Hoogsteen") in Scheme 7. We were able to detect these hydrogen bonds by NMR spectroscopy for the self-complementary duplex d(**2**-dT)$_6$.[20] However, we can not yet identify them in

Table 4 T_m Values and thermodynamic data of oligonucleotide duplexes with nucleosides **3a** or **6a** as dangling ends[a]

Duplex	T_m/°C	$\Delta H°$/kcal mol^{-1}	$\Delta S°$/cal mol^{-1} K^{-1}	$\Delta G°_{310}$/kcal mol^{-1}
5'-d(TAG GTC AAT ACT) (**16**) 3'-d(ATC CAG TTA TGA) (**17**)	47	−86	−245	−10.5
5'-d(**3a**TAG GTC AAT ACT) (**36**) 3'-d(ATC CAG TTA TGA) (**17**)	49	−104	−298	−11.6
5'-d(**3a**TAG GTC AAT ACT) (**36**) 3'-d(ATC C**3a**G TTA TGA) (**24**)	39	−69	−196	−8.2
5'-d(**3a**TAG GTC AAT ACT) (**36**) 3'-d(ATC C**3a**G TT**3a** TGA) (**27**)	29	−59	−171	−6.2
5'-d(**6a** TAG GTC AAT ACT) (**37**) 3'-d(ATC CAG TTA TGA) (**17**)	49	−97	−275	−11.6
5'-d(**6a** TAG GTC AAT ACT) (**37**) 3'-d(ATC C**6a**G TTA TGA) (**29**)	39	−83	−242	−8.1
5'-d(**6a** TAG GTC AAT ACT) (**37**) 3'-d(ATC C**6a**G TT**6a** TGA) (**33**)	37	−81	−235	−7.9

[a] Data measured at 260 nm in 0.1 M NaCl, 10 mM $MgCl_2$, and 10 mM Na-cacodylate buffer (pH 7.0), with 5 μM + 5 μM oligonucleotide concentration.

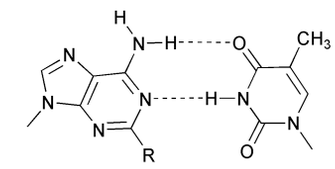

IIIa: cl^{2}A$_d$-dT, R = Cl
IIIb: n^{2}A-dT, R = NH_2

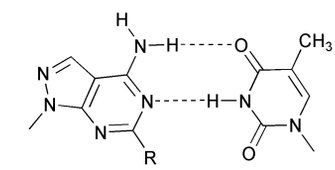

IVa: **6b**-dT, R = Cl
IVb: **4**-dT, R = NH_2

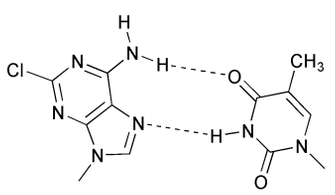

V: cl^{2}A$_d$-dT

Scheme 6 Base pair motifs **III**–**V**.

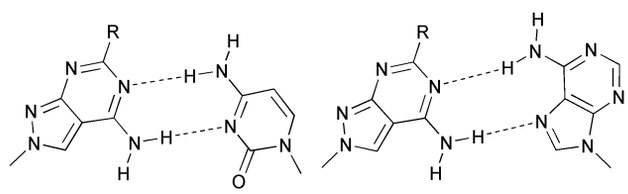

VIa: **1**-dC, R = NH_2
VIb: **2**-dC, R = H
VIc: **3b**-dC, R = Cl

VIIa: **1**-dA, R = NH_2
VIIb: **2**-dA, R = H
VIIc: **3b**-dA, R = Cl

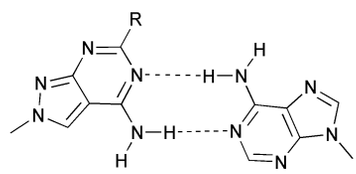

VIIIa: **1**-dA, R = NH_2
VIIIb: **2**-dA, R = H
VIIIc: **3b**-dA, R = Cl

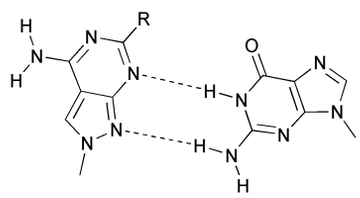

IXa: **1**-dG, R = NH_2
IXb: **2**-dG, R = H
IXc: **3b**-dG, R = Cl

Scheme 7 Base pair motifs **VI**–**IX**.

non-self-complementary duplexes with a single incorporation of the nucleoside **2**.

Now, the nucleoside **3a**, not containing an amino group, and the 2-chloronucleoside **3b** were used as chemical probes for the hydrogen bonded base pair motifs of **1** or **2**. The thermal stabilities of oligonucleotide duplexes containing **3a** should confirm the importance of hydrogen bonds involving the amino groups during the formation of ambiguous base pairs formed by compounds **1** or **2**. Oligonucleotide duplexes incorporating **3b** were expected to show an increased stability over that of **2** as was found for the 7-substituents of regularly linked 8-aza-7-deazapurine nucleosides.[14] The former is a direct consequence of the base pair motifs **VIc**, **VIIc**, **VIIIc**, **IXc** (Scheme 7) locating the 2-substituents in the major groove.

Compounds **3a**,**b** were incorporated into oligonucleotides and hybridized with complementary strands incorporating the four canonical DNA-constituents opposite to the modification position (Table 5). According to the T_m values neither compound **3a** nor **3b** shows the universal base pairing properties of the nucleosides **1** or **2**.[2,3] Compound **3a** forms more stable duplexes when it is incorporated opposite to dG, while the 2-chloro nucleoside **3b** leads to two sets of duplexes showing similar stabilities. Those with compound **3b** located opposite to dC or dA are significantly more stable than those opposite to dG or dT. The $\triangle T_m$ between the two series is about 5–10 °C. On the other hand, all duplexes are more stable than those with the abasic residue S. The results discussed for **3a** support the formation of H-bonded base pairs of **1** or **2** shown in Scheme 5. According to these base pair motifs the 2-chloro substituents of the nucleoside **3b** are located in the major groove of all the four universal base pairs motifs. When **3b** forms base pairs with dC

Table 5 T_m Values and thermodynamic data of duplex formation of oligonucleotides containing nucleosides **3a** and **3b** opposite to the canonical nucleosides[a,b]

Duplex	T_m/°C	$\Delta H°$/kcal mol^{-1}	$\Delta S°$/cal mol^{-1} K^{-1}	$\Delta G°_{310}$/kcal mol^{-1}
5′-d(TAG GTC A**3a**T ACT) (**20**) 3′-d(ATC CAG T**T**A TGA) (**17**)	39	−79	−225	−8.6
5′-d(TAG GTC A**3a**T ACT) (**20**) 3′-d(ATC CAG T**C**A TGA) (**38**)	35	−69	−200	−7.4
5′-d(TAG GTC A**3a**T ACT) (**20**) 3′-d(ATC CAG T**A**A TGA) (**39**)	38	−67	−190	−8.0
5′-d(TAG GTC A**3a**T ACT) (**20**) 3′-d(ATC CAG T**G**A TGA) (**40**)	43	−81	−229	−9.6
5′-d(TAG GTC A**3b**T ACT) (**21**) 3′-d(ATC CAG T**T**A TGA) (**17**)	40	−76	−216	−8.4
5′-d(TAG GTC A**3b**T ACT) (**21**) 3′-d(ATC CAG T**C**A TGA) (**38**)	46	−83	−233	−10.3
5′-d(TAG GTC A**3b**T ACT) (**21**) 3′-d(ATC CAG T**A**A TGA) (**39**)	46	−81	−227	−10.1
5′-d(TAG GTC A**3b**T ACT) (**21**) 3′-d(ATC CAG T**G**A TGA) (**40**)	41	−77	−221	−8.8
5′-d(TAG G**T**C AAT ACT) (**16**) 3′-d(ATC C**3a**G TTA TGA) (**24**)	40	−65	−180	−8.6
5′-d(TAG G**C**C AAT ACT) (**41**) 3′-d(ATC C**3a**G TTA TGA) (**24**)	36	−69	−197	−7.7
5′-d(TAG G**A**C AAT ACT) (**42**) 3′-d(ATC C**3a**G TTA TGA) (**24**)	39	−65	−184	−8.2
5′-d(TAG G**G**C AAT ACT) (**43**) 3′-d(ATC C**3a**G TTA TGA) (**24**)	43	−69	−194	−9.0
5′-d(TAG G**T**C AAT ACT) (**16**) 3′-d(ATC C**3b**G TTA TGA) (**25**)	39	−80	−231	−8.2
5′-d(TAG G**C**C AAT ACT) (**41**) 3′-d(ATC C**3b**G TTA TGA) (**25**)	47	−101	−289	−11.0
5′-d(TAG G**A**C AAT ACT) (**42**) 3′-d(ATC C**3b**G TTA TGA) (**25**)	46	−89	−254	−10.3
5′-d(TAG G**G**C AAT ACT) (**43**) 3′-d(ATC C**3b**G TTA TGA) (**25**)	37	−67	−192	−7.8
5′-d(TAG GTC A**S**T ACT) (**44**) 3′-d(ATC CAG TTA TGA) (**17**)	33	−47	−129	−7.0
5′-d(TAG GTC A**S**T ACT) (**44**) 3′-d(ATC CAG T**C**A TGA) (**38**)	34	−52	−146	−7.1
5′-d(TAG GTC A**S**T ACT) (**44**) 3′-d(ATC CAG T**A**A TGA) (**39**)	34	−51	−141	−7.2
5′-d(TAG GTC A**S**T ACT) (**44**) 3′-d(ATC CAG T**G**A TGA) (**40**)	33	−48	−131	−7.0
5′-d(TAG G**T**C AAT ACT) (**16**) 3′-d(ATC C**S**G TTA TGA) (**45**)	33	−61	−174	−6.9
5′-d(TAG G**C**C AAT ACT) (**41**) 3′-d(ATC C**S**G TTA TGA) (**45**)	35	−65	−187	−7.4
5′-d(TAG G**A**C AAT ACT) (**42**) 3′-d(ATC C**S**G TTA TGA) (**45**)	35	−76	−222	−7.2
5′-d(TAG G**G**C AAT ACT) (**43**) 3′-d(ATC C**S**G TTA TGA) (**45**)	40	−71	−202	−8.6

[a] Data measured at 260 nm in 1 M NaCl, 100 mM $MgCl_2$, and 60 mM Na-cacodylate buffer (pH 7.0) with 5 μM + 5 μM oligonucleotide. [b] dS, 1, 2-dideoxyribose.[2]

or dA, the 2-chloro substituent can be well accommodated in the major groove and has enough steric freedom during its interaction with the substituents of the cognate base. As a result, the T_m value increases. However, the increase is rather small (1–2 °C). The situation is different when **3b** tends to form base pairs with dT or dG. Now, the 2-chloro substituents clash with the oxo groups of dT or dG resulting in 3–7 °C lower T_m values.

When the regularly linked nucleosides **6a** and **6b** were paired with dC, dA, and dG, the thermal stabilities of the duplexes were always lower than those of duplexes containing dT (Table 6). The behavior of **6a** and **6b** is similar to purine nucleosides, but different from the unusually linked regioisomers **3a** and **3b**. The CD-spectra of duplexes containing normal or modified nucleosides **3a**,**b** and **6a**,**b** (data not shown) show only minor changes compared to the unmodified duplex **16·17**. This demonstrates that there is only little disturbance of the B-type duplex structure.

4. Base pairing of regularly and unusually linked nucleosides in self-complementary duplexes. We have already reported on the high duplex stability of self-complementary duplexes incorporating compounds **1** or **2** alternating with dT compared to those containing dA (Table 7). As it is known that oligonucleotide duplexes formed by dA–dT base pairs show a very particular structure with a poor base overlap of the dA–dT units,[21,22] this overlap is apparently increased in the case of the oligonucleotide duplexes incorporating unusually linked nucleosides.[6] Thus, oligonucleotide duplexes incorporating the unusually linked nucleosides form an autonomous DNA structure which develop stronger base stacking (base pairs **I** and **IIa**, Scheme 5). Oligonucleotide **48** incorporating the 2-chloro

Table 6 T_m Values and thermodynamic data of duplex formation of oligonucleotides containing nucleosides **6a** and **6b** opposite to the canonical nucleosides[a]

Duplex	T_m/°C	$\Delta H°$/kcal mol^{-1}	$\Delta S°$/cal mol^{-1} K^{-1}	$\Delta G°_{310}$/kcal mol^{-1}
5′-d(TAG GTC A**6a**T ACT) (**28**) 3′-d(ATC CAG T**T**A TGA) (**17**)	44	−82	−235	−9.6
5′-d(TAG GTC A**6a**T ACT) (**28**) 3′-d(ATC CAG T**C**A TGA) (**38**)	34	−67	−193	−7.2
5′-d(TAG GTC A**6a**T ACT) (**28**) 3′-d(ATC CAG T**A**A TGA) (**39**)	36	−70	−199	−7.7
5′-d(TAG GTC A**6a**T ACT) (**28**) 3′-d(ATC CAG T**G**A TGA) (**40**)	34	−57	−161	−7.3
5′-d(TAG GTC A**6b**T ACT) (**30**) 3′-d(ATC CAG T**T**A TGA) (**17**)	44	−76	−213	−9.5
5′-d(TAG GTC A**6b**T ACT) (**30**) 3′-d(ATC CAG T**C**A TGA) (**38**)	31	−58	−166	−6.7
5′-d(TAG GTC A**6b**T ACT) (**30**) 3′-d(ATC CAG T**A**A TGA) (**39**)	38	−71	−203	−8.1
5′-d(TAG GTC A**6b**T ACT) (**30**) 3′-d(ATC CAG T**G**A TGA) (**40**)	38	−60	−167	−7.9
5′-d(TAG G**T**C AAT ACT) (**16**) 3′-d(ATC C**6a**G TTA TGA) (**29**)	39	−78	−224	−8.2
5′-d(TAG G**C**C AAT ACT) (**41**) 3′-d(ATC C**6a**G TTA TGA) (**29**)	35	−73	−210	−7.3
5′-d(TAG G**A**C AAT ACT) (**42**) 3′-d(ATC C**6a**G TTA TGA) (**29**)	38	−68	−194	−8.0
5′-d(TAG G**G**C AAT ACT) (**43**) 3′-d(ATC C**6a**G TTA TGA) (**29**)	39	−66	−187	−8.3
5′-d(TAG G**T**C AAT ACT) (**16**) 3′-d(ATC C**6b**G TTA TGA) (**31**)	46	−86	−243	−10.2
5′-d(TAG G**C**C AAT ACT) (**41**) 3′-d(ATC C**6b**G TTA TGA) (**31**)	35	−67	−191	−7.4
5′-d(TAG G**A**C AAT ACT) (**42**) 3′-d(ATC C**6b**G TTA TGA) (**31**)	40	−78	−223	−8.6
5′-d(TAG G**G**C AAT ACT) (**43**) 3′-d(ATC C**6b**G TTA TGA) (**31**)	41	−73	−208	−8.7

[a] Data measured at 260 nm in 1 M NaCl, 100 mM $MgCl_2$, and 60 mM Na-cacodylate buffer (pH 7.0) with 5 μM + 5 μM oligonucleotide.

Table 7 T_m Values and thermodynamic data of self-complementary duplexes containing nucleosides **1**, **2**, **3b**, **6b** and 2-chloro-2′-deoxyadenosine[a,b]

Duplex	T_m/°C	$\Delta H°$/kcal mol^{-1}	$\Delta S°$/cal mol^{-1} K^{-1}	$\Delta G°_{310}$/kcal mol^{-1}
[5′-d(**1T1T1T1T1T1T**1T)-3′]$_2$ (**46·46**)	58	−72	−192	−11.3
[5′-d(**2T2T2T2T2T2T**)-3′]$_2$ (**47·47**)	49	−74	−207	−9.6
[5′-d(**3bT3bT3bT3bT3bT3bT**)-3′]$_2$ (**48·48**)	—	—	—	—
[5′-d(**6bT6bT6bT6bT6bT6bT**)-3′]$_2$ (**49·49**)	—	—	—	—
[5′-d(ATATATATATAT)-3′]$_2$ (**50·50**)	33	−50	−139	−6.3
[5′-d(A*TA*TA*TA*TA*TA*T)-3′]$_2$ (**51·51**)	33			

[a] Data measured at 260 nm in 1 M NaCl, 100 mM $MgCl_2$,and 60 mM Na-cacodylate buffer (pH 7.0) with 5 μM + 5 μM oligonucleotide. [b] A* (cl^2A_d) = 2-chloro-2′-deoxyadenosine.

nucleoside **3b** does not form a self-complementary duplex for the reason already discussed above. This observation strongly supports the base pair motifs shown in Scheme 5 (base pair **IIb**, Scheme 5), at least for the base pair with dT, and probably also for that with dG. It was also observed that the oligonucleotide **49** incorporating the regularly linked nucleoside **6b** does not form a duplex at all, which is in line with the Watson–Crick base pair motif **IVa** (Scheme 6) leading also to a clash of the 2-chloro substituent. Contrary to the pyrazolo[3,4-*d*]pyrimidine nucleoside **6b**, the 2-chloro-2′-deoxyadenosine (A*) forms a duplex (**51·51**) as stable as that of d(A–T)$_6$ (**50·50**), a finding reported earlier from our laboratory (Table 7).[23] The only structural difference between **6b** and 2-chloro-2′-deoxyadenosine is the transposition of the nitrogen from position 7 to position 8. As a consequence, position 7 is no longer a proton acceptor site. Thus, compound **6b** cannot form a Hoogsteen base pair, while such a base pair is formed during the duplex formation of oligonucleotides incorporating 2-chloro-2′-deoxyadenosine (motif **V**, Scheme 6). Such selective Hoogsteen base pairing should always occur when the adenine moiety carries a bulky substituent. Other examples on this matter have been already reported.[17,24,25]

Conclusions

Compounds **3a**,**b** incorporated in oligonucleotides were used as structural probes to study the base pairing properties of the universal nucleosides **1** and **2**. The absence of amino groups in compound **3a** results in labile duplexes when this nucleoside is positioned opposite the four canonical DNA constituents. This demonstrates the existence of hydrogen bonds in the ambiguous base pairs of the universal nucleosides **1** and **2**. When the 2-chloro nucleoside **3b** replaced **1** or **2** at the same positions as **3a** two sets of duplexes were formed (i) those with high T_m values with **3b** opposite dA or dC and (ii) low T_m duplexes with **3b** opposite dG or dT. The decrease of the base pair stability results from the steric hindrance of the 2-chloro substituent of **3b** with the oxo group of dG or dT within the novel reverse

Watson–Crick or Hoogsteen-like base pairs. On the other hand the 2-chloro substituents are well accommodated in the base pairs formed with dA or dC. Both observations are in accordance with the suggested base pair motifs. Similar to **3b** the regularly linked nucleoside **6b** does not form base pairs in self-complementary or non-self-complementary duplexes which results from the steric hindrance of the bulky 2-chloro substituents within the minor groove. Different from **6b**, 2-chloro-2′-deoxyadenosine has been shown to form stable base pairs with dT. This results from a reorientation of the Watson–Crick to Hoogsteen base pair motif thereby releasing the strain caused by the bulky 2-substituent. As a result, the exclusive formation of a Hoogsteen DNA motif is observed in self-complementary oligonucleotide duplexes when 2-chloro-2′-deoxyadenosine alternates with dT.

Experimental

General

All chemicals were purchased from Aldrich, Sigma, Fluka (Sigma-Aldrich Chemie GmbH, Deisenhofen, Germany), or Glen Research (Sterling, VA, USA). Solvents were of laboratory grade and were distilled before use. Thin-layer chromatography (TLC): aluminum sheets, silica gel 60 F_{254}, 0.2 mm layer (Merck, Germany). Column flash chromatography (FC): silica gel 60 (Merck, Germany) at 0.5 bar (5×10^4 Pa); sample collection with an UltraRac-II fractions collector (LKB Instruments, Bromma, Sweden). UV spectra: U-3200-UV/VIS spectrometer (Hitachi, Japan). CD spectra: Jasco 600 spectropolarimeter (Jasco, Tokio, Japan) with a temperature controller Lauda RCS 6 and a water bath Lauda RK 20 (Lauda Germany); 1 cm cuvettes. NMR spectra: Avance DPX-250 or AMX-500 spectrometers (Bruker, Germany) at 250.13 and 500.14 MHz (^{1}H), 125.13 (^{13}C) and 101.3 MHz (^{31}P); chemical shifts δ are in ppm relative to $SiMe_4$ as internal standard or external 85% H_3PO_4, J values are given in Hertz.

Oligonucleotides

Synthesis, purification and analysis

The oligodeoxyribonucleotides were synthesized with a DNA synthesizer model 392 B (Applied Biosystems, Weiterstadt, Germany) on a 1 μmol scale. The syntheses followed the regular protocol of the DNA synthesizer for phosphoramidites using the trityl-on mode.[3] After cleavage from the solid support, the oligonucleotides were deprotected in 25% aq. NH_3 solution for 3 h at RT. After evaporation, the residues were subjected to HPLC (RP-18, 250 × 4 mm, Merck, Germany) on a Merck-Hitachi HPLC apparatus. The purification was carried out according to the methods described in ref. 2: Eluents: 0.1 M $(Et_3NH)OAc$ (pH 7.0)–MeCN 95 : 5 (A) and MeCN (B); Gradient for trityl-on oligonucleotides: 3 min 15% A in B, 12 min 20–40% A in B (A, MeCN; B, 0.1 M $(Et_3NH)OAc$ (pH 7.2)–MeCN 95 : 5), 1 mL/min. The purified trityl-on oligonucleotides were detritylated with 2.5% dichloroacetic acid for 5 min at 0 °C, and then purified by HPLC again using the following gradient: 20 min, 0–20% A in B with flow rate of 1 mL min^{-1}. The oligonucleotides were desalted *via* HPLC (RP-18, silica gel), inorganic material was eluted with H_2O, while the oligonucleotides were eluted with MeOH–H_2O (3 : 2, v/v) and lyophilised on a Speed-Vac evaporator and stored at –24 °C.

MALDI-TOF was recorded on a Biflex-III spectrometer (Bruker, Leipzig, Germany) in the reflector mode. The average power of the nitrogen laser (337.1 nm) at 20 Hz was 3–4 mW (150–200 μJ pulse^{-1}) with a delay time of 600 ns. All measurements were performed using a positive detection mode with the following parameters: dwell time: 1.00 ns, delay: 40 000 ns, Uisl: 19.00 kV, Uis2: 15.80 kV, Urefl: 20.00 kV, Ulens: 9.35 kV. The spectra were obtained by overlaying 500–1000 single pulses with a cutoff mass of 1000 Da. The spectrometer was calibrated using an oligonucleotide calibration standard (Bruker, Part No. 206200) containing a 12-mer (3645.44 Da), a 20-mer (6117.04 Da) and a 30-mer (9191.03 Da).

The samples for measurement were prepared on Scout MTP MALDI targets (Bruker): 1 μL of the supernatant of a saturated solution of recrystallized 3-hydroxypicolinic acid in doubly distilled H_2O containing BioRad microbeads AG 50W-X8 (100–200 mesh, NH_4^+-form) was spotted on a target well. A suspension (1 μL) containing 15–20 microbeads in H_2O was added followed by 1 μL of an aq. oligonucleotide solution (concentration: 0.1 A_{260} units per 10 μL H_2O) The mixture was carefully dried on the target, and the microbeads were removed mechanically with a tip.

T_m Measurements

T_m Values of the thermal dissociation/association of the duplexes were measured by temperature-dependent UV-melting profiles with a Cary-1E UV/VIS spectrophotometer (Varian, Australia) equipped with a Cary thermoelectrical controller; the actual temperature was measured in the reference cell with a Pt-100 resistor. The thermodynamic data of duplex formation were calculated using the program MeltWin.[26] The molar absorption coefficients of the nucleoside constituents at λ_{260} nm: A_d 15400, C_d 7300, G_d 11500, T_d 8800, **3a** 6000, **3b** 6800, **6a** 3500, **6b** 5300.

1-[2-Deoxy-3,5-di-*O*-(*p*-toluoyl)-β-D-*erythro*-pentofuranosyl]-1*H*-pyrazolo[3,4-*d*]pyrimidine 11a. To a stirred suspension of compound **8a**[6] (3.0 g, 25.0 mmol) in MeCN (200 mL) powdered KOH (4.2 g, 75 mmol) was added at RT. After 10 min of stirring, TDA-1 (1.2 mL) was added, and stirring was continued for another 15 min. 1-Chloro-2-deoxy-3,5-di-*O*-(*p*-toluoyl)-α-D-*erythro*-pentofuranose **9**[7] (12.7 g, 32.7 mmol) was added in portions. The reaction was continued for 10 min, the solution was filtered, concentrated, adsorbed on silica gel and loaded onto a silica gel column. Flash chromatography (FC) with a petroleum ether–EtOAc mixture (10 : 1 ⟶ 4 : 1) gave two zones. From the first zone a colorless solid was isolated (4.1 g, 35%) (Found: C, 66.23; H, 5.10; N, 11.85%. $C_{26}H_{24}N_4O_5$ requires C, 66.10; H, 5.08; N, 11.86%); TLC (silica gel, petroleum ether–EtOAc 2 : 1) R_f 0.43; λ_{max} (MeOH/nm) (ε/dm^3 mol^{-1} cm^{-1}) 241 (33000); δ_H (250.13 MHz; [d$_6$]DMSO; $SiMe_4$) 2.34, 2.40 (6 H, s, 2 × CH_3), 2.93, 3.20 (2 H, m, 2′-H), 4.53 (2 H, m, 5′-H), 4.70 (1 H, m, 4′-H), 5.90 (1 H, m, 3′-H), 6.76 (1 H, t, J 5.7, 1′-H), 7.21–7.96 (8 H, m, 2 × Ph), 8.97 (1 H, s, 3-H), 9.04 (1 H, s, 6-H), 9.47 (1 H, s, 4-H).

2-[2-Deoxy-3,5-di-*O*-(*p*-toluoyl)-β-D-*erythro*-pentofuranosyl]-2*H*-pyrazolo[3,4-*d*]pyrimidine 10a. The second zone from the above glycosylation furnished **10a** (0.9 g, 8%) as a colorless solid (Found: C, 66.15; H, 5.15; N, 11.76%. $C_{26}H_{24}N_4O_5$ requires C, 66.09; H, 5.12; N, 11.86%); TLC (silica gel, petroleum ether–EtOAc 2 : 1) R_f 0.12; λ_{max} (MeOH/nm) (ε/dm^3 mol^{-1} cm^{-1}) 241 (32000); δ_H (250.13 MHz; [d$_6$]DMSO; $SiMe_4$) 2.34, 2.40 (6 H, 2s, 2 × CH_3); 2.91, 3.23 (2 H, 2m, 2′-H), 4.53 (2 H, m, 5′-H), 4.69 (1 H, m, 4′-H), 5.89 (1 H, m, 3′-H), 6.76 (1 H, t, J 5.7, 1′-H), 7.21–7.96 (8 H, m, 2 × Ph), 8.97 (1 H, s, 3-H), 9.03 (1 H, s, 6-H), 9.46 (1 H, s, 4-H).

2-(2-Deoxy-β-D-*erythro*-pentofuranosyl)-2*H*-pyrazolo[3,4-*d*]-pyrimidine 3a. The solution of compound **10a** (1.1 g, 2.3 mmol) in 0.1 M ^{i}PrONa in ^{i}PrOH (100 mL) was stirred at RT for 2 h. The solution was neutralized with glacial acetic acid, concentrated, and adsorbed on silica gel for FC with CH_2Cl_2–MeOH (20 : 1 ⟶ 10 : 1) to obtain compound **3a** as a colorless solid (0.51 g, 93%) (Found: C, 50.76; H, 5.22; N, 23.82%. $C_{10}H_{12}N_4O_3$ requires C, 50.84; H, 5.12; N, 23.72%); TLC (silica gel, CH_2Cl_2–

MeOH, 9 : 1) R_f 0.13; λ_{max} (MeOH/nm) (ε/dm^3 mol^{-1} cm^{-1}) 206 (28700), 271 (8600); δ_H (250.13 MHz; [d$_6$]DMSO; SiMe$_4$) 2.46, 2.61 (2 H, m, 2′-H), 3.59 (2 H, 2 m, 5′-H), 3.95 (1 H, m, 4′-H), 4.00 (1 H, m, 3′-H), 4.97 (1 H, t, 5′-OH), 5.38 (1 H, d, 3′-OH), 6.47 (1 H, t, 1′-H), 8.97 (1 H, s, 3-H), 9.00 (1 H, s, 6-H), 9.48 (1 H, s, 4-H).

1-(2-Deoxy-β-D-*erythro*-pentofuranosyl)-1*H*-pyrazolo[3,4-*d*]-pyrimidine 6a. Compound **11a** (3.0 g, 6.3 mmol) was deprotected in 0.1 M ^{i}PrONa in ^{i}PrOH (300 mL) in the same manner as described for compound **10a**. Purification by FC with CH_2Cl_2–MeOH (20 : 1 ⟶ 10 : 1) yields compound **6a** as a colorless solid (1.35 g, 90%) (Found: C, 50.96; H, 5.24; N, 23.72%. $C_{10}H_{12}N_4O_3$ requires C, 50.84; H, 5.12; N, 23.72%); TLC (silica gel, CH_2Cl_2–MeOH, 9 : 1) R_f 0.22; λ_{max} (MeOH/nm) (ε/dm^3 mol^{-1} cm^{-1}) 209 (32000), 261 (4000); δ_H (250.13 MHz; [d$_6$]DMSO; SiMe$_4$) 2.36, 2.89 (2 H, 2 m, 2′-H), 3.39, 3.54 (2 H, 2 m, 5′-H), 3.84 (1 H, m, 4′-H), 4.49 (1 H, m, 3′-H), 4.73 (1 H, t, *J* 5.7, 5′-OH), 5.34 (1 H, d, *J* 4.5, 3′-OH), 6.74 (1 H, t, *J* 6.4, 1′-H), 8.47 (1 H, s, 3-H), 9.05 (1 H, s, 6-H), 9.36 (1 H, s, 4-H).

2-[2-Deoxy-5-*O*-(4,4′-dimethoxytriphenylmethyl)-*β*-D-*erythro*-pentofuranosyl-2*H*-pyrazolo[3,4-*d*]pyrimidine 12a. Compound **3a** (0.4 g, 1.69 mmol) was dried by repeated coevaporation with anhydrous pyridine (3 × 5 mL) and dissolved in anhydrous pyridine (1.5 mL). $(MeO)_2TrCl$ (0.66 g, 1.94 mmol) was added to the solution in portions. After stirring for 3 h at RT, the solution was diluted with CH_2Cl_2 (50 mL), washed with 5% aq. $NaHCO_3$ (2 × 15 mL) and brine (1 × 15 mL). The solution was dried with anhydrous Na_2SO_4, filtered and evaporated. The residue was subjected to FC with a CH_2Cl_2–MeOH mixture (20 : 1 ⟶ 15 : 1) affording a colorless solid (0.85 g, 94%) (Found: C, 68.88; H, 5.45; N, 10.28%. $C_{31}H_{30}N_4O_5$ requires C, 69.13; H, 5.61, N, 10.40%); TLC (silica gel, CH_2Cl_2–MeOH, 9 : 1) R_f 0.46; λ_{max} (MeOH/nm) (ε/dm^3 mol^{-1} cm^{-1}), 234 (23000), 272 (10600); δ_H (250.13 MHz; [d$_6$]DMSO; SiMe$_4$) 2.45, 2.73 (2 H, 2 m, 2′-H), 3.17 (2 H, m, 5′-H), 3.69 (6 H, s, 2 × CH_3O), 4.06 (1 H, m, 4′-H), 4.53 (1 H, m, 3′-H), 5.43 (1 H, m, 3′-OH), 5.54 (1 H, m, 1′-H), 6.51–7.31 (13 H, m, 3 × Ph), 8.89 (1 H, s, 3-H), 8.99 (1 H, s, 6-H), 9.42 (1 H, s, 4-H).

1-[2-Deoxy-5-*O*-(4,4′-dimethoxytriphenylmethyl)-β-D-*erythro*-pentofuranosyl]-1*H*-pyrazolo[3,4-*d*]pyrimidine 13a. A solution of compound **6a** (1.0 g, 4.23 mmol) in anhydrous pyridine (2.0 mL) was treated with $(MeO)_2TrCl$ (1.87 g, 5.51 mmol) in an analogous way as described for **12a**. Compound **13a** was isolated after FC as a colorless solid (2.1 g, 92%) (Found: C, 69.56; H, 5.78; N, 10.64%. $C_{31}H_{30}N_4O_5$ requires C, 69.13; H, 5.61; N, 10.40%); TLC (silica gel, CH_2Cl_2–MeOH, 9 : 1) R_f 0.2; λ_{max} (MeOH/nm) (ε/dm^3 mol^{-1} cm^{-1}), 234 (23000), 274 (6700); δ_H (250.13 MHz; [d$_6$]DMSO; SiMe$_4$) 2.40, 2.85 (2 H, 2 m, 2′-H), 3.05 (2 H, m, 5′-H), 3.69, 3.70 (6 H, 2 s, 2 × CH_3O), 3.98 (1 H, m, 4′-H), 4.60 (1 H, m, 3′-H), 5.38 (1 H, m, 3′-OH), 6.68–7.30 (14 H, m, 1′-H, 3 × Ph), 8.41 (1 H, s, 3-H), 9.09 (1 H, s, 6-H), 9.37 (1 H, s, 4-H).

2-[2-Deoxy-5-*O*-(4,4′-dimethoxytriphenylmethyl)-β-D-*erythro*-pentofuranosyl]-2*H*-pyrazolo[3,4-*d*]pyrimidine 3′-(2-cyanoethyl diisopropylphosphoramidite) 14a. To a stirred and degassed solution of compound **12a** (0.54 g, 1.0 mmol) in anhydrous dichloromethane (20 mL) were added diisopropylethylamine (0.36 mL, 2.07 mmol) and 2-cyanoethyl diisopropylphosphoramidochloridite (0.36 mL, 1.61 mmol) under an argon atmosphere. After stirring for 30 min at RT the solution was diluted with CH_2Cl_2 (50 mL), washed with a 5% aq. $NaHCO_3$ (2 × 20 mL) and brine (1 × 20 mL), and was dried with anhydrous Na_2SO_4. After filtration and evaporation the residue was subjected to FC with CH_2Cl_2–$(CH_3)_2CO$ (15 : 1) yielding compound **14a** (0.42 g, 57%) as a colorless foam. TLC (silica gel, CH_2Cl_2–$(CH_3)_2CO$, 10 : 1) R_f 0.23, 0.40; δ_H (250.13 MHz; [d$_6$]DMSO; SiMe$_4$) 1.19 (12 H, m, 2 × CH(CH_3)$_2$); 2.46, 2.63 (2 H, 2 m, 2′-H), 2.78, 2.93 (2 H, 2 m, 2 × CH(CH$_3$)$_2$), 3.54–3.75 (4 H, m, CH_2CH_2), 3.80 (6 H, s, 2 × CH_3O), 4.35 (1 H, m, 4′-H), 4.74 (1 H, m, 3′-H), 6.45 (1 H, m, 1′-H), 6.78–6.83, 7.23–7.39 (13 H, 2m, 3 × Ph), 8.56, 8.61 (1 H,2 s, 3-H), 9.07 (1 H, s, 6-H), 9.09, 9.11 (1 H, 2 s, 4-H). δ_P (101.25 MHz; $CDCl_3$; H_3PO_4) 150.4, 150.8.

1-[2-Deoxy-5-*O*-(4,4′-dimethoxytriphenylmethyl)-*β*-D-*erythro*-pentofuranosyl]-1*H*-pyrazolo[3,4-*d*]pyrimidine 3′-(2-cyanoethyl diisopropylphosphoramidite) 15a. Starting with compound **13a** (0.81 g, 1.5 mmol) in anhydrous CH_2Cl_2 (20 mL) diisopropylethylamine (0.54 mL, 3.10 mmol) and 2-cyanoethyl diisopropylphosphoramidochloridite (108 μL, 0.48 mmol) were added as described for **14a**. Compound **15a** was obtained after FC with a mixture of CH_2Cl_2–$(CH_3)_2CO$ (15 : 1) and gave a colorless foam (0.8 mg, 72%); TLC (silica gel, CH_2Cl_2–$(CH_3)_2CO$, 10 : 1) R_f 0.67, 0.76; δ_H (250.13 MHz; [d$_6$]DMSO; SiMe$_4$) 1.24 (12 H, m, 2 × CH(CH_3)$_2$), 2.49–3.81 (8 H, m, 2′-H, 2 × CH(CH$_3$)$_2$, CH_2CH_2), 3.78 (6 H, s, 2 × CH_3O), 4.28 (1 H, m, 4′-H), 4.95 (1 H, m, 3′-H), 6.91 (1 H, m, 1′-H), 6.71–6.76, 7.17–7.40 (13 H, 2m, 3 × Ph), 8.10 (1 H, 2 s, 3-H); 9.07 (1 H, s, 6-H), 9.19 (1 H, 2 s, 4-H); δ_P (101.25 MHz; $CDCl_3$; H_3PO_4) 149.8, 149.9.

6-Chloro-4-isopropoxy-1*H*-pyrazolo[3,4-*d*]pyrimidine 8b. A solution of 4,6-dichloro-1*H*-pyrazolo[3,4-*d*]pyrimidine **7**[8] (7.7 g, 40.7 mmol) in sodium isopropoxide in isopropanol (1 M, 500 mL) was stirred for 1 h at RT. The solution was neutralized with glacial acidic acid, concentrated, adsorbed on silica gel, and loaded on a silica gel column. FC with CH_2Cl_2–MeOH (20 : 1 ⟶ 15 : 1) furnished a colorless solid (6.0 g, 69%) (Found: C, 45.51; H, 4.18; N, 26.54%. $C_8H_9ClN_4O$ requires C, 45.19; H, 4.27; N, 26.35%); TLC (silica gel, CH_2Cl_2–MeOH, 15 : 1) R_f 0.27; λ_{max} (MeOH/nm) (ε/dm^3 mol^{-1} cm^{-1}) 252 (9700); δ_H (250.13 MHz; [d$_6$]DMSO; SiMe$_4$) 1.41 (6 H, s, (CH_3)$_2$CH), 5.53 (1 H, m, (CH$_3$)$_2$CH), 8.23 (1 H, s, 3-H), 14.11 (1 H, br s, NH).

6-Chloro-1-[2-deoxy-3,5-di-*O*-(*p*-toluoyl)-β-D-*erythro*-pentofuranosyl]-4-isopropoxy-1*H*-pyrazolo[3,4-*d*]pyrimidine 11b. To a stirred mixture of 6-chloro-4-isopropoxy-1*H*-pyrazolo[3,4-*d*]-pyrimidine **8b** (0.58 g, 2.7 mmol) and KOH (0.62 g, 11.1 mmol) in MeCN (50 mL) TDA-1 (0.1 mL) was added. After 10 min 1-chloro-2-deoxy-3,5-di-*O*-toluoyl-α-D-*erythro*-pentofuranose **9** (1.3 g, 3.3 mmol) was added in portions. The mixture was stirred for 10 min and filtered. The filtrate was concentrated, adsorbed on silica gel and applied to FC with a petroleum ether–EtOAc mixture (20 : 1 ⟶ 10 : 1). The first zone furnished **11b** as a colorless foam (0.76 g, 49%) (Found: C, 61.59; H, 5.13; N, 9.91%. $C_{29}H_{29}ClN_4O_6$ requires C, 61.65; H, 5.17; N, 9.92%); TLC (silica gel, petroleum ether–EtOAc, 4 : 1) R_f 0.58; λ_{max}(MeOH/nm) (ε/dm^3 mol^{-1} cm^{-1}) 242 (34600). δ_H (250.13 MHz; [d$_6$]DMSO; SiMe$_4$) 1.39, 1.42 (6 H, 2 s, (CH_3)$_2$CH), 2.37, 2.40 (6 H, 2 s, 2 × CH_3O), 2.80, 3.27 (2 H, 2 m, 2′-H), 4.35–4.58 (3 H, m, 4′-H, 5′-H), 5.54 (1 H, m, (CH$_3$)$_2$CH), 5.85 (1 H, m, 3′-H), 6.77 (1 H, t, *J* 5.95, 1′-H), 6.75–7.97 (8 H, m, arom. H), 8.38 (1 H, s, 3-H).

6-Chloro-2-[2-deoxy-3,5-di-*O*-(*p*-toluoyl)-β-D-*erythro*-pentofuranosyl]-4-isopropoxy-2*H*-pyrazolo[3,4-*d*]pyrimidine 10b. The second zone of above glycosylation gave compound **10b** as a colorless foam (0.5 g, 32%) (Found: C, 61.72; H, 5.22; N, 9.94%. $C_{29}H_{29}ClN_4O_6$ requires C, 61.65; H, 5.17; N, 9.92%); TLC (silica gel, petroleum ether–EtOAc mixture, 4 : 1) R_f 0.27; λ_{max}(MeOH/nm) (ε/dm^3 mol^{-1} cm^{-1}) 226 (25000), 241 (29300). δ_H (250.13 MHz; [d$_6$]DMSO; SiMe$_4$) 1.36, 1.39 (6 H, 2 s, (CH_3)$_2$CH), 2.35, 2.40 (6 H, 2 s, 2 × CH_3O), 2.88, 3.19 (2 H, 2 m, 2′-H), 4.43–4.67 (3 H, m, 4′-H, 5′-H), 5.51 (1 H, m, (CH$_3$)$_2$CH), 5.88 (1 H, m,

3′-H), 6.57 (1 H, dd, *J* 4.37, 6.58, 1′-H), 7.21–7.94 (8 H, m, arom. H), 8.87 (1 H, s, 3-H).

4-Amino-6-chloro-1-(2-deoxy-β-D-*erythro*-pentofuranosyl)-1*H*-pyrazolo[3,4-*d*]pyrimidine 6b. A suspension of compound **11b** (1.56 g, 2.76 mmol) in MeOH saturated with dry ammonia (200 mL) was stirred in a sealed flask for two days at RT. The clear solution was concentrated and adsorbed on silica gel and applied to FC with a CH_2Cl_2–MeOH mixture (20 : 1 ⟶ 10 : 1). Compound **6b** was isolated as a colorless solid (0.75 g, 95%); TLC (silica gel, CH_2Cl_2–MeOH mixture, 15 : 1) R_f 0.19; λ_{max}(MeOH/nm) (ε/dm^3 mol^{-1} cm^{-1}) 274 (8700). δ_H (250.13 MHz; [d_6]DMSO; $SiMe_4$) 2.24, 2.76 (2 H, 2 m, 2′-H), 3.39, 3.47 (2 H, 2 m, 5′-H), 3.79 (1 H, m, 4′-H), 4.41 (1 H, m, 3′-H), 4.72 (1 H, t, *J* 5.76, 5′-OH), 5.27 (1 H, d, *J* 4.70, 3′-OH), 6.44 (1 H, t, *J* 6.36, 1′-H), 8.15 (1 H, s, 3-H), 8.34, 8.54 (2 H, 2 s, NH_2).

4-Amino-6-chloro-2-(2-deoxy-β-D-*erythro*-pentofuranosyl)-2*H*-pyrazolo[3,4-*d*]pyrimidine 3b. A suspension of **10b** (1.05 g, 1.86 mmol) in ammonia-saturated MeOH (100 mL) was stirred in a sealed vessel for two days at RT. Concentration and purification by FC with CH_2Cl_2–MeOH (20 : 1 ⟶ 15 : 1) furnished **3b** as a colorless solid (0.5 g, 94%) (Found: C, 42.00; H, 4.23; N, 24.24%. $C_{10}H_{12}ClN_5O_3$ requires C, 42.04; H, 4.23; N, 24.51%); TLC (silica gel, CH_2Cl_2–MeOH, 15 : 1) R_f 0.1; λ_{max}(MeOH/nm) (ε/dm^3 mol^{-1} cm^{-1}) 269 (7975), 287 (9300). δ_H (250.13 MHz; [d_6]DMSO; $SiMe_4$) 2.34, 2.58 (2 H, 2 m, 2′-H), 3.47, 3.53 (2 H, 2 m, 5′-H), 3.90 (1 H, m, 4′-H), 4.38 (1 H, m, 3′-H), 4.87 (1 H, t, *J* 5.56, 5′-OH), 5.34 (1 H, d, *J* 4.40, 3′-OH), 6.30 (1 H, t, *J* 6.38, *J* 5.26, 1′-H), 8.18, 8.32 (2 H, 2 s, NH_2), 8.54 (1 H, s, 3-H).

6-Chloro-2-(2-deoxy-β-D-*erythro*-pentofuranosyl)-4-{[(di-*n*-butylamino)methylidene]amino}-2*H*-pyrazolo[3,4-*d*]pyrimidine 12b. A stirred solution of compound **3b** (0.4 g, 1.4 mmol) in MeOH (20 mL was treated with *N,N*-di-*n*-butylformamide dimethyl acetal (2.1 mL) at RT for 3 h. The solution was evaporated and the residue was subjected to FC with a mixture of CH_2Cl_2–MeOH (20 : 1 ⟶ 15 : 1)). Compound **12b** was isolated as a colorless foam (0.46 g, 77%) (Found: C, 53.70; H, 7.00; N, 19.80%. $C_{19}H_{29}ClN_6O_3$ requires C, 53.70; H, 6.88; N, 19.78%); TLC (silica gel, CH_2Cl_2–MeOH (9 : 1) R_f 0.44; λ_{max}(MeOH/nm) (ε/dm^3 mol^{-1} cm^{-1}) 244 (8200), 338 (30000). δ_H (250.13 MHz; [d_6]DMSO; $SiMe_4$) 0.92 (6 H, m, 2 × CH_3), 1.31 (4 H, m, 2 × CH_2), 1.59 (4 H, m, 2 × CH_2), 2.38, 2.59 (2 H, 2 m, 2′-H), 3.62 (6 H, m, 2 × CH_2, 5′-H), 3.90 (1 H. m, 4′-H), 4.41 (1 H, m, 3′-H), 4.95 (1 H, t, *J* 5.5, 5′-OH), 5.36 (1 H, d, *J* 4.4, 3′-OH), 6.33 (1 H, t, *J* 5.8, 1′-H), 8.72 (1 H, s, 3-H), 8.85 (1 H, s, CH=N).

6-Chloro-1-(2-deoxy-β-D-*erythro*-pentofuranosyl)-4-{[(dimethylamino)methylidene]amino}-1*H*-pyrazolo[3,4-*d*]pyrimidine 13b. A solution of compound **6b** (0.15 g, 0.5 mmol) in MeOH (10 mL) was stirred with *N,N*-dimethylformamide dimethyl acetal (1.2 mL, 8.96 mmol) at 40 °C for 6 h. The solution was evaporated, and the residue was subjected to FC with a mixture of CH_2Cl_2–MeOH (20 : 1 ⟶ 15 : 1) to give compound **13b** as a colorless solid (155 mg, 87%) (Found: C, 44.96; H, 4.92; N, 24.71%. $C_{13}H_{17}ClN_6O_3$ requires C, 45.82; H, 5.03; N, 24.66%); TLC (silica gel, CH_2Cl_2–MeOH mixture, 15 : 1) R_f 0.13; λ_{max}(MeOH/nm) (ε/dm^3 mol^{-1} cm^{-1}) 238 (11100), 317 (31000). δ_H (250.13 MHz; [d_6]DMSO; $SiMe_4$) 2.28, 2.80 (2 H, 2 m, 2′-H), 3.19, 3.27 (6 H, 2 s, 2 × CH_3), 3.35, 3.49 (2 H, 2 m, 5′-H), 3.80 (1 H, m, 4′-H), 4.41 (1 H, m, 3′-H), 4.73 (1 H, t, *J* 5.7, 5′-OH), 5.30 (1 H, d, *J* 4.9, 3′-OH), 6.50 (1 H, t, *J* 6.3, 1′-H), 8.19 (1 H, s, 3-H), 8.87 (1 H, s, CH=N).

6-Chloro-2-[2-deoxy-5-*O*-(4,4′-dimethoxytriphenylmethyl)-β-D-*erythro*-pentofuranosyl]-4-{[(di-*n*-butylamino)methylidene]-amino}-2*H*-pyrazolo[3,4-*d*]pyrimidine 12c. Compound **12b** (0.26 g, 0.61 mmol) was dried by co-evaporation with anhydrous pyridine and dissolved in anhydrous pyridine (2 mL). To the stirred solution was added $(MeO)_2TrCl$ (0.36 g, 1.06 mmol), and the stirring continued for 1 h. The work-up procedure was the same as described for **12a** yielding compound **12c** as a colorless foam (0.35 g, 79%) (Found: C, 66.14; H, 6.62; N, 11.50%. $C_{40}H_{47}ClN_6O_5$ requires C, 66.06; H, 6.51; N, 11.56%); TLC (silica gel, CH_2Cl_2–MeOH, 15 : 1) R_f 0.43; λ_{max}(MeOH/nm) (ε/dm^3 mol^{-1} cm^{-1}) 283 (8640), 338 (28900). δ_H (250.13 MHz; [d_6]DMSO; $SiMe_4$) 0.89 (6 H, m, 2 × CH_3), 1.28 (4 H, m, 2 × CH_2), 1.58 (4 H, m, 2 × CH_2), 2.38, 2.68 (2 H, 2 m, 2′-H), 3.09 (4 H, m, 2 × CH_2), 3.51 (4 H, m, CH_2, 5′-H), 3.68, 3.70 (6 H, 2 s, 2 × MeO), 3.99 (1 H, m, 4′-H), 4.49 (1 H, m, 3′-H), 5.40 (1 H, d, *J* 4.9, 3′-OH), 6.38 (1 H, m, 1′-H), 6.73–7.32 (13 H, m, arom. H), 8.67(1 H, s, 3-H), 8.84 (1 H, s, CH=N).

6-Chloro-1-[2-deoxy-5-*O*-(4,4′-dimethoxytriphenylmethyl)-β-D-*erythro*-pentofuranosyl]-4-{[(dimethylamino)methylidene]-amino}-1*H*-pyrazolo[3,4-*d*]pyrimidine 13c. To a stirred solution of compound **13b** (0.4 g, 1.2 mmol) in anhydrous pyridine (2 mL) was added $(MeO)_2TrCl$ (0.53 g, 1.56 mmol) which was worked up in an analogous way as described for **12a**. Compound **13c** was obtained as a colorless foam (0.51 g, 68%) (Found: C, 63.36; H, 5.40; N, 12.98%. $C_{34}H_{35}ClN_6O_5$ requires C, 63.50; H, 5.49; N, 13.07%); TLC (silica gel, CH_2Cl_2–MeOH, 15 : 1) R_f 0.11; λ_{max}(MeOH/nm) (ε/dm^3 mol^{-1} cm^{-1}) 235 (28300), 317 (30100). δ_H (250.13 MHz; [d_6]DMSO; $SiMe_4$) 2.33, 2.75 (2 H, 2 m, 2′-H), 3.03 (4 H, m, CH_2, 5′-H), 3.27, 3.33 (6 H, 2 s, 2 × CH_3), 3.69, 3.70 (6 H, 2 s, 2 × MeO), 3.92 (1 H, m, 4′-H), 4.54 (1 H, m, 3′-H), 5.33 (1 H, d, *J* 5.13, 3′-OH), 6.53 (1 H, m, 1′-H), 6.52–7.48 (13 H, m, arom. H), 8.13 (1 H, s, 3-H), 8.87 (1 H, s, CH=N).

6-Chloro-2-[2-deoxy-5-*O*-(4,4′-dimethoxytriphenylmethyl)-β-D-*erythro*-pentofuranosyl]-4-{[(di-*n*-butylamino)methylidene]-amino}-2*H*-pyrazolo[3,4-*d*]pyrimidine 3′-(2-cyanoethyl diisopropylphosphoramidite) 14b. To a stirred and degassed solution of compound **12c** (0.3 g, 0.41 mmol) in anhydrous CH_2Cl_2 (20 mL) were added diisopropylethylamine (0.16 mL, 0.92 mmol) and 2-cyanoethyl diisopropylphosphoramidochloridite (160 μL, 0.72 mmol) at RT under an Ar atmosphere. The stirring was continued for 30 min and the reaction mixture was worked-up as described for compound **14a**. Colorless foam (310 mg, 81%); TLC (silica gel, CH_2Cl_2–$(Me)_2CO$, 15 : 1) R_f 0.33, 0.49; δ_H (250.13 MHz; [d_6]DMSO; $SiMe_4$) 0.89–1–35 (10 H, m, 2 × CH_3, 2 × CH_2), 1.71 (4 H, m, 2 × CH_2), 2.42, 2.92 (2 H, 2 m, 2′-H), 2.65 (4 H, m, 2 × CH_2), 3.28–3.91 (13 H, m, 2 × CH_2, CH, 5′-H, 2 × MeO), 4.32 (1 H, m, 4′-H), 4.89 (1 H, m, 3′-H), 6.29 (1 H, m, 1′-H), 6.75–7.40 (13 H, m, arom. H), 8.38 (1 H, s, 3-H), 8.87 (1 H, s, CH=N). δ_P (101.25 MHz; $CDCl_3$; H_3PO_4): 150.3, 150.5.

6-Chloro-1-[2-deoxy-5-*O*-(4,4′-dimethoxytriphenylmethyl)-β-D-*erythro*-pentofuranosyl]-4-{[(dimethylamino)methylidene]-amino}-1*H*-pyrazolo[3,4-*d*]pyrimidine 3′-(2-cyanoethyl) diisopropylphosphoramidite) 15b. Starting with a solution of compound **13c** (0.28 g, 0.44 mmol) in anhydrous CH_2Cl_2 (20 mL) diisopropylethylamine (0.16 mL, 0.92 mmol) and 2-cyanoethyl diisopropylphosphoramidochloridite (160 μL, 0.72 mmol) were added at RT. The work up was the same as described for compound **14a** to give **15b** as a colorless foam (0.31 g, 84%); TLC (silica gel, CH_2Cl_2–$(Me)_2CO$, 15 : 1) R_f 0.45, 0.57; δ_H (250.13 MHz; [d_6]DMSO; $SiMe_4$) 2.48, 2.65 (2 H, 2 m, 2′-H), 3.22 (4 H, m, 2 × CH_2), 3.26 (6 H, 2 s, 2 × CH_3), 3.45–3.94 (12 H, m, 5′-H, 2 × MeO, 2 × CH_2), 4.22 (1 H, m, 4′-H), 4.87 (1 H, m, 3′-H), 7.45–6.73 (14 H, m, 1′-H, arom. H), 8.05 (1 H, s, 3-H), 8.88 (1 H, s, CH=N). δ_P (101.25 MHz; $CDCl_3$; H_3PO_4): 149.6, 149.7.

Acknowledgements

We thank Dr Helmut Rosemeyer and Dr Yang He for the NMR measurements, Miss Elisabeth Feiling for oligonucleotide

synthesis, and Mr Khalil Shaikh for MALDI-TOF spectra. We also appreciate a generous gift of 5,7-dihydro-1*H*-pyrazolo-[3,4-*d*]pyrimidin-4,6-(5*H*,7*H*)-dione by Mr Anup Jawalekar. Financial support by the Roche Diagnostics, GmbH is gratefully acknowledged.

References

1 F. Seela, M. Zulauf and H. Debelak, *Helv. Chim. Acta*, 2000, **83**, 1437–1453.
2 F. Seela and H. Debelak, *Nucleic Acids Res.*, 2000, **28**, 3224–3232.
3 J. He and F. Seela, *Helv. Chim. Acta*, 2002, **85**, 1340–1354.
4 H. Steker, PhD Thesis, Paderborn, 1988.
5 F. Seela and S. Menkhoff, *Liebigs Ann. Chem.*, 1986, 1213–1221.
6 Z. Kazimierczuk, R. Mertens, W. Kawczynski and F. Seela, *Helv. Chim. Acta*, 1991, **74**, 1742–1748.
7 F. Seela and K. Kaiser, *Helv. Chim. Acta*, 1988, **71**, 1813–1823.
8 M. Hoffer, *Chem. Ber.*, 1960, **93**, 2777–2781.
9 R. K. Robins, *J. Am. Chem. Soc.*, 1957, **79**, 6407–6415.
10 Y. S. Sanghvi, G. D. Hoke, S. M. Freier, M. C. Zounes, C. Gonzalez, L. Cummins, H. Sasmor and P. D. Cook, *Nucleic Acids Res.*, 1993, **21**, 3197–3203.
11 J. He, F. Seela, H. Eickmeier and H. Reuter, *Acta Crystallogr., Sect. C: Cryst. Struct. Commun.*, 2002, **58**, o593–o595.
12 T. Sato, *Acta Crystallogr., Sect. C: Cryst. Struct. Commun.*, 1984, **40**, 880–882.
13 F. Seela and M. Zulauf, *J. Chem. Soc., Perkin Trans 1*, 1999, 479–488.
14 F. Seela and G. Becher, *Nucleic Acids Res.*, 2001, **29**, 2069–2078.
15 J. He and F. Seela, *Tetrahedron*, 2002, **58**, 4535–4542.
16 P. Hentosh and J. C. McCastlain, *Nucleic Acids Res.*, 1991, **19**, 3143–3148.
17 J. Sagi, E. Szakonyi, M. Vorlickova and J. Kypr, *J. Biomol. Struct. Dyn.*, 1996, **13**, 1035–1041.
18 F. Seela and A. Jawalekar, *Helv. Chim. Acta*, 2002, **85**, 1857–1868.
19 H. Rosemeyer and F. Seela, *J. Chem. Soc., Perkin Trans 2*, 2002, 746–750.
20 M. German, personal communication.
21 F. Seela and T. Wenzel, *Helv. Chim. Acta*, 1994, **77**, 1485–1499.
22 S. Brahms, V. Fritsch, J. G. Brahms and E. Westhof, *J. Mol. Biol.*, 1992, **223**, 455–476.
23 N. Ramzaeva and F. Seela, *Chem. Res. Toxicol.*, 1994, **7**, 643–649.
24 T. Hakoshima, T. Fukui, M. Ikehara and K.-I. Tomita, *Proc. Natl. Acad. Sci. USA*, 1981, **78**, 7309–7313.
25 K. Liu, H. T. Miles, J. Frazier and V. Sasisekharan, *Biochemistry*, 1993, **32**, 11802–11809.
26 J. A. McDowell and D. H. Turner, *Biochemistry*, 1996, **35**, 14077–14089.